IVYSPRING INTERNATIONAL PUBLISHER

Theranostics

2018; 8(8): 2289-2299. doi: 10.7150/thno.23483

Research Paper

Paper-based electrochemiluminescence sensor for highly sensitive detection of amyloid-β oligomerization: Toward potential diagnosis of Alzheimer's disease

Hongxing Liu, Xiaoming Zhou✉, Qi Shen and Da Xing ✉

MOE Key Laboratory of Laser Life Science & Institute of Laser Life Science, College of Biophotonics, South China Normal University, Guangzhou, China

✉ Corresponding authors: E-mail: xingda@scnu.edu.cn and E-mail: zhouxm@scnu.edu.cn; Tel: +86-20-85210089; Fax: +86-20-85216052

Received: 2017.10.25; Accepted: 2018.02.04; Published: 2018.03.11

Abstract

Development of a rapid and sensitive method for Aβ(1–42) aggregation detection is of great importance to overcome the limitations of conventional techniques. In this study, we developed a label-free paper-based electrochemiluminescence sensor for amyloid-β aggregation detection toward potential diagnosis of Alzheimer's disease (AD). The paper-based chip used in the system serves as a low-cost and disposable detection method. In this detection platform, the bonding of $[Ru(phen)_2dppz]^{2+}$ to Aβ(1-42) aggregates results in enhanced electrochemiluminescence due to the change in the polarity of the microenvironment when $[Ru(phen)_2dppz]^{2+}$ intercalated into the β-sheets during oligomerization. The oligomerization process of Aβ(1-42) can be monitored in real time by the novel method, and as low as 100 pM equivalent monomer concentration of Aβ(1-42) could be detected simultaneously. In addition, the cerebrospinal fluid of transgenic AD model mice was tested by this method, which is highly consistent with genetic identification. In addition, we demonstrated that this detection platform could be a potential new method for the screening of Aβ(1-42) aggregation inhibitors, highlighting the practical application capacity of this platform. The platform is label free, low cost and sensitive. Therefore, the proposed platform holds great promise for the diagnosis of AD.

Key words: Aβ(1–42) aggregation, electrochemiluminescence, $[Ru(phen)_2dppz]^{2+}$, paper-based bipolar electrode, Alzheimer's disease

Introduction

Alzheimer's disease (AD) is a fatal progressive neurodegenerative disease that affects over 35 million individuals globally [1, 2]. To date, there are no specific vaccines or other effective preventive measures for this disease [3]. AD is accompanied by cognitive decline, memory loss, and behavioral disability and is usually associated with the generation of neuritic plaques and neurofibrillary tangles in the brain. Previous studies have demonstrated that the major component of the neuritic plaques is the β-amyloid peptide (Aβ), which comprises 39–43 amino acid residues that are cleaved from the amyloid precursor protein [4]. Among the Aβ isoforms that are present in AD, Aβ(1–42) aggregates are widely believed to be the most pathogenic, and the aggregation of Aβ(1–42) into oligomers and fibrils is a key process associated with AD [5, 6]. Thus, Aβ(1–42) aggregation is generally considered an important biomarker and drug target for AD research and therapy.

Clinical and research evidence indicates that the neuropathology starts 10−20 years before AD becomes clinically overt. Patients who are clinically diagnosed with AD are usually in the middle and late stages of the disease, and the existing treatments are inadequate for achieving satisfactory efficacy. An assay of aggregated Aβ(1–42) in the early stages of AD can help diagnose AD in an early stage and can help

researchers understand the pathogenesis of the disease [7]. Thus, the detection of Aβ(1–42) oligomerization may be a potential approach for the early diagnosis of AD.

A range of methods with high reproducibility and reliability have been employed to detect Aβ(1–42) aggregation, including imageology-based methods [2, 8] such as computerized X-ray tomography (CT) and magnetic resonance imaging (MRI), fluorescence correlation spectroscopy (FCS) [9], surface plasmon resonance (SPR) [10], aggregation-induced emission (AIE)-based fluorescence assay methods [11, 12], polyacrylamide gel electrophoresis (PAGE) [13], immunoprecipitation [14], mass spectrometry [15], thioflavin T (ThT)-based fluorescent staining [16-18], and enzyme-linked immunosorbent assay (ELISA) [19]; however, they usually suffer from requiring expensive instruments and complicated operations, thereby limiting their applications to routine testing for Aβ(1–42) aggregation. Alternatively, to overcome these problems, electrochemical techniques have been used to monitor Aβ(1–42) aggregation [20, 21]. Although these assays have shown low detection limits, some challenges still exist. For instance, the electrode usually requires a sophisticated surface modification process. Therefore, it is necessary to construct a label-free, low-cost yet sensitive sensor for Aβ(1–42) aggregation detection.

Recently, we reported a paper-based bipolar electrode electrochemiluminescence (pBPE-ECL) detection system integrating the "light switch" molecule $[Ru(phen)_2dppz]^{2+}$ into the system for sensitive, quantitative, and label-free detection of analytes [22]. In this system, the pBPE was made by wax-screen printing and screen printing. Two driving electrodes of the pBPE were connected to a DC power supply, while the working electrode does not need to be connected to a wire, enabling a wireless assay. We have demonstrated that the "light switch" molecule shows no ECL in aqueous solution but does display intense ECL in the presence of DNA. It has also been reported by other groups that the interaction of $[Ru(phen)_2dppz]^{2+}$ with Aβ(1–42) aggregation may also result in a change in the polarity of the microenvironment in a similar fashion to its interaction with DNA [23-29]. Therefore, we hypothesize that a pBPE-ECL system coupled with the mechanism of $[Ru(phen)_2dppz]^{2+}$ binding to Aβ(1–42) aggregates may facilitate the development of a label-free and sensitive platform for Aβ(1–42) aggregation detection toward the potential diagnosis of AD.

As a proof of concept, for the first time, we developed a label-free and disposable pBPE-ECL sensor for Aβ(1–42) aggregation detection. Compared to reported sensors for Aβ(1–42) aggregation, the proposed approach possesses some remarkable features: 1) The pBPE-ECL detection platform is label free and easy to operate without using expensive instruments [30, 31]; 2) the paper-based detection chip is disposable, low-cost and amenable to batch fabrication [32, 33]; and 3) the detection platform is so sensitive that as low as 100 pM equivalent monomer concentration of Aβ(1-42) could be detected, and the oligomerization process of Aβ(1-42) can be monitored in real time by the novel method simultaneously. The cerebrospinal fluid (CSF) of transgenic AD model mice was tested, and the results were highly consistent with genetic identification, highlighting the practical application capacity of this platform. In addition, we demonstrated the feasibility of this platform as a potential new method for the screening of Aβ aggregation inhibitors. Overall, this platform holds great promise as a potential method for AD diagnosis.

Methods

Materials

1,1,1,3,3,3-Hexafluoroisopropanol (HFIP), thioflavin T and dimethyl sulfoxide (DMSO) were purchased from Sigma-Aldrich (USA). Aβ(1-42), human (>95%) was purchased from ChinaPeptides (Shanghai, China). Whatman chromatography paper (Φ=125.0 mm, pure cellulose paper) was purchased from Hangzhou WoHua Filter Paper Co., Ltd. (Zhejiang, China). Conductive carbon ink (model number CNB-7, <60 Ω square^{-1}), which was used as a fabrication material for the driving/working electrodes, was obtained from Xuzhou Bohui New Materials Technology Co., Ltd. (Xuzhou, China). Solid wax was obtained from a local department store. $[Ru(phen)_2dppz](PF_6)_2$ was synthesized and characterized according to previously reported methods (**Figure S1**). Tripropylamine (TPrA) (≥98%) was obtained from Sigma-Aldrich (St. Louis, MO, USA).

Deionized water was prepared with a water purification system (≥18 MΩ) and used in all the experiments. All the chemical reagents were of analytical reagent grade and were used without any further purification.

Apparatus

A DC power supply (Model LW-K605D) was purchased from Longwei Instrument Meter Co., Ltd. (Hong Kong, China). The voltage of the photomultiplier tube (PMT; MP-962, Perkin Elmer, Wiesbaden, Germany) was set to 850 V for detection. The signal was then amplified and discriminated with transistor-transistor logic (TTL) and quantified using a multi-function acquisition card (PCI-1751, Advantech, Taiwan) controlled by a LabVIEW-based

software program that was configured in-house.

Treatment of Aβ(1-42) Solution

Aβ(1-42) was prepared as previously described [34]: first, lyophilized peptides were dissolved in 220 μL of HFIP, and then the obtained monomeric Aβ(1-42) solution (1 mg/mL) was incubated overnight at room temperature for 24 h. The HFIP solvent was evaporated under nitrogen gas, and the monomeric Aβ(1-42) was redissolved in 44 μL of DMSO. The resultant Aβ(1-42) monomer solution (5 mM) was stored at −20 °C as a stock solution. Aβ(1-42) aggregates were obtained by incubation of the Aβ(1-42) monomer solution in PBS at 37 °C in the dark for more than 24 h.

Atomic force microscopy (AFM) imaging

AFM images of samples withdrawn at different incubation times were studied to directly observe and monitor the formation of fibrils. Tapping mode was used to observe morphologies during the fibrillation process. To scan the AFM images, aliquots of samples withdrawn at different incubation times were diluted with PBS, drop-coated on a freshly cleaved mica surface, and allowed to dry for at least 1 h.

ThT binding fluorescence assay

For real-time detection of Aβ(1–42) aggregation with a ThT binding assay, 50 nM monomeric Aβ(1-42) incubated with PBS buffer (pH 7.4) for 0, 0.5, 1, 2, 4, 8, 16, 24, 48, 72 and 120 h at 37 °C was analyzed using a JASCO-FP6500 LS-55 fluorescence spectrophotometer (PerkinElmer, USA). When screening for Aβ(1–42) aggregation inhibitors with the ThT binding assay, 50 nM monomeric Aβ(1-42) was incubated with different concentrations of Congo red and curcumin ranging from 0 to 100 μM in PBS (pH 7.4) for 24 h at 37 °C. The final concentration of ThT was 6 μM. The excitation wavelength was 440 nm, and the emission intensity at 482 nm was used for analysis.

Collection of CSF from the cisterna magna in mice

The present study was performed in accordance with the guidelines of the Guide for the Care and Use of Laboratory Animals (Institute of Laboratory Animal Resources, Commission on Life Sciences, National Research Council). It was approved by the Institutional Animal Care and Use Committee of our university (South China Normal University, Guang-zhou, China).

CSF samples were taken from the cisterna magna of mice using a method that was published previously with slight modification [35]. Briefly, the mice ere anesthetized with pentobarbital sodium (2 wt%). The skin of the neck was shaved, and the mice were then placed prone on the stereotaxic instrument. A sagittal incision of the skin was made inferior to the occiput. Under the dissection microscope, the subcutaneous tissue and neck muscles through the midline were bluntly separated. Hemostatic forceps were used to hold the muscles apart. Then, the mouse was laid down so that the body made a 135° angle with the fixed head. At this angle, the dura and spinal medulla were visible and had a characteristic glistening and clear appearance, and the circulatory pulsation of the medulla (i.e., a blood vessel) and adjacent CSF space could be seen (**Figure S5A**). The dura was then penetrated with a 6 cm long glass capillary that had a tapered tip with an outer diameter of 0.5 mm. Following a noticeable change in resistance to the capillary insertion, the CSF flows into the capillary (**Figure S5B**). The average volume of CSF obtained was approximately 5 μL. All samples were stored in polypropylene tubes at -80 °C until analysis.

Western blot analysis using β-amyloid antibody to evaluate the amyloid-β oligomer in CSF

Briefly, 5 μL of CSF sample was mixed with SDS sample loading buffer, boiled for 8 min, and separated by 15% SDS-PAGE. Proteins separated in the gels were electrophoretically transferred to PVDF membranes. Membranes were blocked for 1 h using 5% non-fat dry milk in TBS containing 0.5% Tween-20 (TBST) and then incubated with β-amyloid antibody (Santa Cruz, sc-28365) at 4 °C overnight. After three washes with TBST, secondary antibody application was performed at RT for 2 h. The signals were detected with an ODYSSEY Infrared Imaging System (LI-COR). The intensity of the Western blot signals was quantified using ImageJ software (National Institutes of Health (NIH), Bethesda, MD), and the results of densitometric analysis are presented as the ratio of protein/GAPDH protein and are compared with the controls and normalized to 1.

Fabrication of the pBPE

The screen-printing fabrication process for the pBPE was performed according to previously reported methods with slight modifications [22, 36, 37]. Briefly, the patterning shapes for screen-printing the pBPE chip were designed using Adobe Illustrator CS6 and then delivered to the local screen printing shop to manufacture the screens initially. The fabrication process of the molds used for screen printing and wax-screen printing is shown in **Figure S6**. Then, the filter paper was cut into a uniform size. Afterwards, the BPE and driving electrodes were fabricated on the hydrophilic channel by a screen printing technique with carbon ink. Finally, the dried

semi-finished product was heated together with the screen at 80 °C for approximately 10 s to melt the wax to produce hydrophobic areas on it with the screen mesh openings, while areas with a cross-linked photosensitive material yielded the hydrophilic channel during the wax-screen printing process.

pBPE-ECL assays

Once the pBPE was fabricated, the pBPE-ECL assays were performed. A typical procedure is described in detail below. The as-prepared pBPE-ECL chip was placed on a 3D-printed substrate, and the pair of driving electrodes was connected to a DC power supply. Then, 25 μL of the assay solution containing 10 μM $[Ru(phen)_2dppz]^{2+}$ and 50 mM TPrA in 0.1 M PBS (pH 7.4) was dropped onto the center of the pBPE. The pBPE chip was placed into a black box. Before the device was powered on, a 30–60 s wait time was necessary to ensure that the entire channel was completely filled with the solution. Next, the DC power supply was turned on, and the ECL at the BPE anodic pole could be obtained. Finally, the ECL emission collected by the PMT was recorded with a LabVIEW-based photon-counting computer program. The maximum luminescence signal was selected as the valid data in the experiments.

Results and discussion

Detection scheme of pBPE-ECL for Aβ(1-42) aggregation

It has been reported that in aqueous solution or in the presence of monomeric Aβ(1-42), the photoluminescence of $[Ru(phen)_2dppz]^{2+}$ is quenched by the protonation of the phenazine N atoms in the excited state. However, its photoluminescence increases by several orders of magnitude in the presence of Aβ(1-42) oligomers and fibrils because the dppz ligand of $[Ru(phen)_2dppz]^{2+}$ is a hydrophobic extended aromatic system that can efficiently hide from water by binding to the hydrophobic cleft formed between Val18 and Phe20 on the surface of Aβ(1-42) oligomers and fibrils; this cleft is parallel to the β-sheet structure axis. At this site, the side chains of Val18 and Phe20 interact with the aromatic ring of dppz through CH–π and π−π interactions, respectively [23-26].

Therefore, we hypothesize that the light-switching ECL properties of $[Ru(phen)_2dppz]^{2+}$ with Aβ(1-42) aggregates is likely similar to its photoluminescence mechanism. $[Ru(phen)_2dppz]^{2+}$ can intercalate in a label-free manner into the β-sheets when Aβ(1-42) gradually aggregates to form oligomers or fibrils. During the intercalation, the $[Ru(phen)_2dppz]^{2+}$-Aβ(1-42) complex produced a change in the polarity of the microenvironment that favored the population of a luminescent state, resulting in intense ECL emission. The greater the number of hydrophobic regions formed in the process of Aβ(1-42) aggregation was, the greater the ECL intensity obtained (**Figure 1A**). In addition, the emission intensity of the ECL is proportional to the $[Ru(phen)_2dppz]^{2+}$-Aβ(1–42) aggregate complex concentration in the presence of excess TPrA, thereby enabling quantitative detection of Aβ(1–42) *in vitro*.

Conventional electrochemical electrodes usually suffer from requiring a wire connected directly to the working electrode, and electrode preparation is also complicated and difficult to control, increasing the complexity of Aβ(1–42) aggregation detection. In this study, the pBPE made by wax-screen printing and screen printing and the two driving electrodes of the pBPE connected to a DC power supply were developed as a wireless and disposable detection platform. Briefly, wax-screen printing was employed to form hydrophilic channels on filter paper [38], and the carbon ink-based bipolar electrode and driving electrodes were screen printed into the channels. Then, the as-prepared pBPE was placed into two 3D-printed substrates to assemble the pBPE chip, and the pair of driving electrodes was connected to a DC power supply. Once the $[Ru(phen)_2dppz]^{2+}$-Aβ(1–42) aggregate complex was formed, the assay solution containing $[Ru(phen)_2dppz]^{2+}$-Aβ(1–42) aggregate complexes and TPrA was then directly applied to the wireless, low-cost, label-free and sensitive pBPE-ECL system to perform the ECL assays. When sufficient voltage is applied between the two ends of the driving electrode, the potential difference between the pBPE and the solution simultaneously drives redox reactions at both poles of the pBPE. As a result, ECL signals, which are generated at the anodic pole of the pBPE, are captured by the PMT and recorded with a LabVIEW-based photon-counting computer program for further analysis. The mechanism of the $[Ru(phen)_2dppz]^{2+}$-Aβ(1–42) aggregation complex reaction with TPrA at the anode of the pBPE is shown in **Figure 1B**. The mechanism of reaction with TPrA was as follows:

$$[Ru(phen)_2dppz]^{2+}\text{- Aβ(1–42) aggregate} - e^- \rightarrow [Ru(phen)_2dppz]^{3+}\text{- Aβ(1–42) aggregation} \quad (1)$$

$$TPrA - e^- \rightarrow TPrA^{\bullet +} \rightarrow TPrA^{\bullet} + H^+ \quad (2)$$

$$[Ru(phen)_2dppz]^{3+}\text{- Aβ(1–42) aggregation} + TPrA^{\bullet} \rightarrow [Ru(phen)_2dppz]^{2+*}\text{- Aβ(1–42) aggregation} + \text{products} \quad (3)$$

$$[Ru(phen)_2dppz]^{2+*}\text{- Aβ(1–42) aggregation} \rightarrow [Ru(phen)_2dppz]^{2+}\text{- Aβ(1–42) aggregation} + h\nu \quad (4)$$

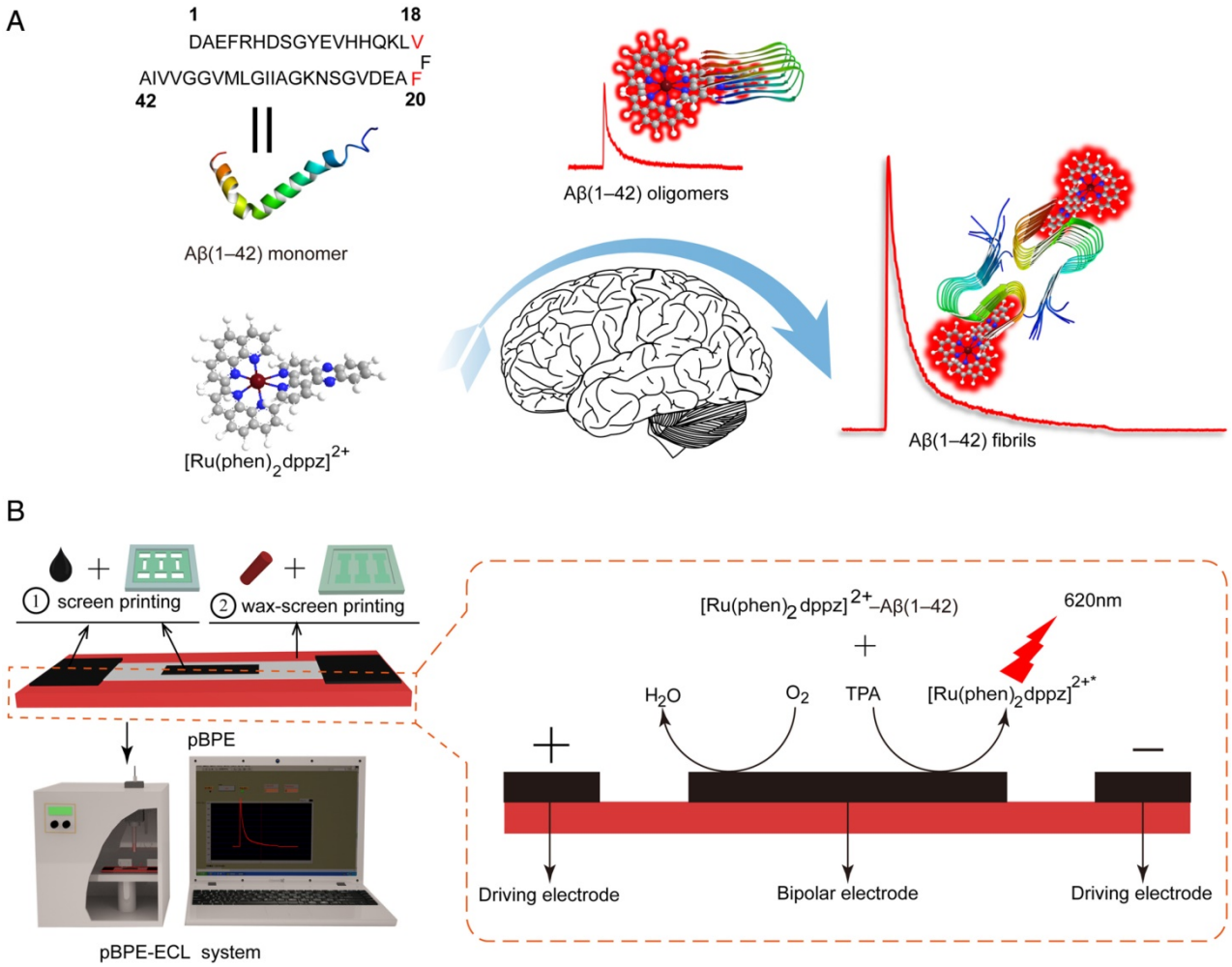

Figure 1. Scheme of the paper-based bipolar electrode electrochemiluminescence sensor for highly sensitive Aβ(1-42) aggregation detection. (A) $[Ru(phen)_2dppz]^{2+}$ was used to monitor the Aβ(1-42) aggregation process. In aqueous solution or in the presence of monomeric Aβ(1-42), the ECL of $[Ru(phen)_2dppz]^{2+}$ is quenched by the protonation of the phenazine N atoms in the excited state. However, its ECL increases by several orders of magnitude in the presence of Aβ(1-42) oligomers and fibrils. The red highlighted letters represent the Val18 and Phe20 sites that $[Ru(phen)_2dppz]^{2+}$ binds to when Aβ(1-42) aggregates form. **(B)** The construction of the pBPE-ECL system and the mechanism of the $[Ru(phen)_2dppz]^{2+}$- Aβ(1–42) aggregate complex reaction with TPrA on the bipolar electrode.

Real-time detection of the Aβ(1–42) aggregation

AD is characterized by an imbalance between the production and clearance of amyloid-β species *in vivo*, while *in vitro*, monomeric Aβ(1-42) presents strong self-aggregation ability and can aggregate into a β-sheet structure of ordered fibrils under specific conditions. The amyloid-β cascade hypothesis suggests that increased Aβ(1-42) aggregation occurs prior to the formation of Aβ oligomers, which is followed by the formation of fibrils and ultimately of plaques. The "light-switch" molecule $[Ru(phen)_2dppz]^{2+}$ was integrated into the pBPE-ECL system to study Aβ(1-42) aggregation in real time. To verify the aggregation degree of Aβ(1-42) by quantitative analysis of pBPE-ECL sensors, 50 nM monomeric Aβ(1-42) was added to 5 mM pH 7.4 PBS at 37 °C, incubated for 0, 0.5, 1, 2, 4, 8, 16, 24, 48, 72 and 120 h, and then mixed with 10 μM $[Ru(phen)_2dppz]^{2+}$ and 50 mM TPrA, followed by application of the mixture solution to the paper-based bipolar electrodes for ECL detection. As seen from the results in **Figure 2A**, the ECL gradually increases over time. The reason for this phenomenon is as follows: the more oligomeric or fibrous Aβ(1-42) is formed with the increasing aggregation of Aβ(1-42), the more hydrophobic regions that $[Ru(phen)_2dppz]^{2+}$ can bind to, thereby resulting in remarkable ECL enhancement.

To demonstrate whether the aggregation is the only reason for the increased ECL intensity, we applied 50 nM monomeric Aβ(1-42) incubated with pH 7.4 PBS for 0, 0.5, 1, 2, 4, 8, 16, 24, 48, 72 and 120 h at 37 °C to a dynamic light scattering assay and a ThT binding fluorescence assay. As seen from the results

in **Figure S1** and **Figure 2B**, the particle size of Aβ(1-42) and the fluorescence intensity gradually increase with time. To intuitively observe the morphology of different forms of Aβ(1-42) and directly corroborate the abovementioned experiments, we incubated monomeric Aβ(1-42) for different times and applied it to AFM analysis. From the experimental results in **Figure 2C**, it can be seen that the morphology of different forms of Aβ(1-42) in AFM is different: the Aβ(1-42) oligomers are spherical or elliptical spherical particles with a height of approximately 25 nm, whereas the Aβ(1-42) fibers showed long fibrous aggregation under the microscope with a height of approximately 10 nm and a length> 1000 nm. The oligomer and aggregated Aβ(1–42) were applied to TEM for further verification. According to the TEM images (**Figure S2**), the oligomer Aβ(1–42) shows a 150 nm spherical shape, while aggregated Aβ(1–42) shows a fibrous shape. The experimental results also directly verified the formation of β-amyloid oligomers/fibrils. The results of this experiment are also consistent with the results of particle size analysis [39]. The ECL experimental results were consistent with other parallel experiments, which well demonstrated the capacity of the paper-based ECL sensor to detect Aβ aggregation in real time *in vitro*.

Sensitivity assay

To validate the sensitivity of our newly developed pBPE-ECL assay system for Aβ(1–42) aggregation detection *in vitro*, different concentrations of monomeric Aβ(1–42) ranging from 50 nM to 50 pM were incubated at 37 °C in pH 7.4 PBS solution for 24 h. There was no direct measurement method to determine the concentration of Aβ(1–42) aggregates. Therefore, we used the initial concentration of Aβ(1–42) monomer as the equivalent concentration of Aβ(1–42) aggregates under the same aggregation condition. The as-prepared Aβ(1–42) aggregates were then incubated with 10 μM $[Ru(phen)_2dppz]^{2+}$ and 50 mM TPrA to evaluate the sensitivity of the pBPE-ECL analysis system. As shown in **Figure 3A**, the ECL intensities increase linearly with increasing monomeric Aβ(1–42) concentration from 50 nM to 50 pM. The maximum luminescence signals corresponding to each concentration of Aβ(1–42) and the negative control are presented in **Figure 3A**. Linear analysis of the experimental results in **Figure 3B** indicates a correlation coefficient (R^2) of 0.99572, which suggests that this system is capable of reliably performing Aβ(1–42) aggregation detection *in vitro*. For n=3, the R.S.D of the present method for Aβ(1–42) aggregation, which is calculated based on standard deviation divided by mean value at each test point, ranges from 3.34% to 9.62%. To define whether a sample is Aβ(1–42)-positive, a cutoff value is calculated based on the following formula:

$$V_{cutoff} = V_{control} + 3V_{stdev(con)} \quad (5)$$

where $V_{control}$ is the average light emission from the negative control without Aβ(1–42) and $V_{stdev(con)}$ represents the standard deviation ($V_{stdev(con)}$) of the ECL reading from the negative control samples. According to this formula, the cutoff level for Aβ(1–42)-positive samples was set at 884 counts/s. An ECL signal less than this value should not be indicated as Aβ(1–42)-positive under our conditions. With the use of our method, the limit of detection (LOD) was determined to be 100 pM (equivalent monomer concentration), which is lower than the reported Aβ(1–42) levels of AD patients.[40]

Transgenic mouse analysis

To further verify that the pBPE-ECL system can be used for actual sample detection, we collected the CSF from mice for direct detection. CSF (~5 μL) was collected from the cisterna magna of C57BL6 wild-type mice and APP/PS1 transgenic AD model mice and then incubated with 30 μL of a mixed solution containing 1x PBS, 10 μM $[Ru(phen)_2dppz]^{2+}$ and 50 mM TPA for 30 min, followed by application to the pBPE-ECL platform for ECL detection. It can be seen from the experimental results (**Figure 4A**) that the maximum luminescence signal of the CSF from the APP/PS1 transgenic AD model mice was significantly higher than that of the CSF from the C57BL6 wild-type mice. Moreover, the mean ECL value of the CSF from APP/PS1 transgenic AD model mice was significantly different from that of the CSF from the C57BL6 wild-type mice ($P < 0.005$) (**Figure 4B**).

The APPswe/PSEN1dE9 (APP/PS1) transgenic mouse model used in this study was obtained by coinjection of mice with the APPswe and PS1dE9 vectors, while the C57BL6 wild-type mice did not harbors these vectors. Thus, we can simply identify the two kinds of mice by amplification of the exogenous genes with PCR. We further identified the mice by designing a pair of APP primers (the length of the amplified product was 377 bp) and a pair of PS1 primers (the length of the amplified product was 608 bp), which were derived from the APPswe and PS1dE9 vectors, respectively (**Figure S3A**), and the total DNA of the transgenic mice and common mice was applied to PCR. The results of electrophoresis (**Figure S3B**) showed that the DNA of the normal C57BL6 mice in lane 2 did not obtain the amplified bands and that the rest of the lanes for the APP/PS1 transgenic AD model mice did gain the expected

amplify bands. The results of the genetic identification are also highly consistent with the results of the ECL experiment. Western blot analysis of CSF samples in **Figure 4C-D** indicated that the protein level of Aβ oligomer in APP/PS1 transgenic mice was significantly higher than that in C57/BL6 wild-type (WT) mice ($P < 0.01$). After identification, we can determine that the pBPE-ECL system can be used not only for pure sample detection but also for actual sample detection with high accuracy.

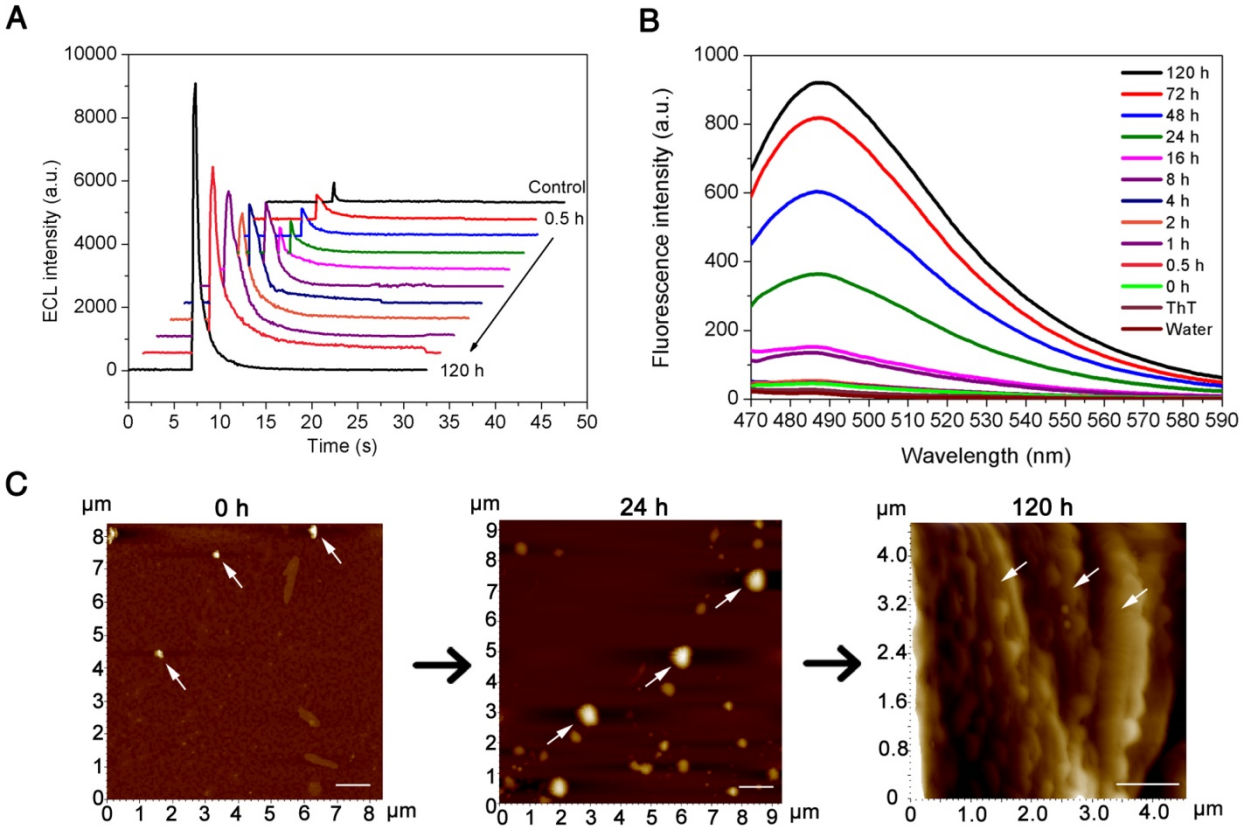

Figure 2. Real-time detection of the Aβ(1–42) aggregation. (A) ECL intensities of 50 nM monomeric Aβ(1–42) incubated at 37 °C in 5 mM pH 7.4 PBS solution for 0, 0.5, 1, 2, 4, 8, 16, 24, 48, 72 and 120 h when applied to an assay solution containing 10 μM $[Ru(phen)_2dppz]^{2+}$ and 50 mM TPrA. **(B)** Thioflavin T (ThT) binding fluorescence assay of 50 nM monomeric Aβ(1–42) incubated at 37 °C in pH 7.4 PBS solution for 0, 0.5, 1, 2, 4, 8, 16, 24, 48, 72 and 120 h. **(C)** AFM images of 50 nM monomeric Aβ(1–42) incubated at 37 °C in PBS, pH 7.4 for 0 h, 24 h, and 120 h, respectively. The scale bar was 1 μm.

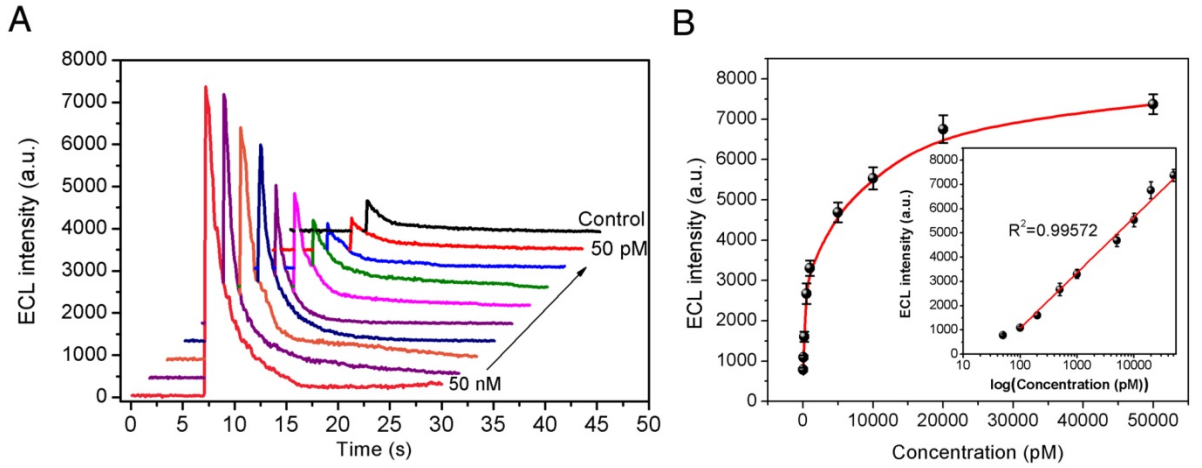

Figure 3. Sensitivity assay. (A) The electrochemiluminescence results on the paper-based bipolar electrode collected by a photomultiplier tube (PMT) with 50 nM, 20 nM, 10 nM, 5 nM, 1 nM, 500 pM, 200 pM, 100 pM, and 50 pM equivalent monomer concentration of Aβ(1–42) and the control experiment result. **(B)** Calibration curve for the Aβ(1–42) aggregation assay using the pBPE-ECL system. The inset shows the linear relationship between ECL intensity and the logarithm of Aβ(1–42) concentrations. ECL assay conditions were as follows: different concentrations of monomeric Aβ(1–42) ranging from 50 pM to 50 nM were first incubated at 37 °C in 5 mM pH 7.4 PBS solution for 24 h and then mixed with 10 μM $[Ru(phen)_2dppz]^{2+}$ and 50 mM TPA for 30 min, and finally, the assay solution was directly applied to the pBPE-ECL system to perform the ECL assays at a driving voltage of 14 V. The error bars represent the standard deviations from three independent experiments.

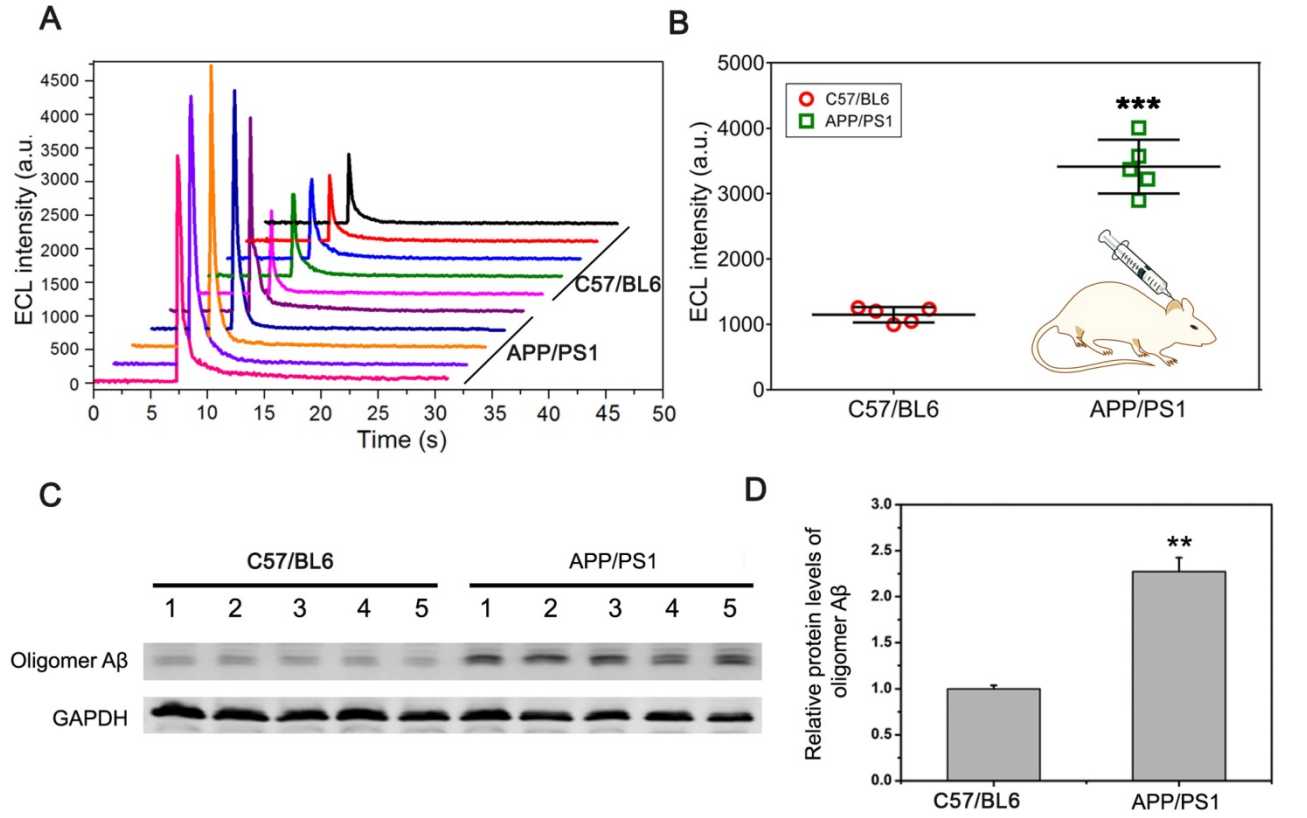

Figure 4. CSF assay using a mouse model. (A) The ECL assay results of ten CSF specimens collected from the cisterna magna of five normal C57BL6 mice and five APP/PS1 transgenic AD model mice. A total of ~5 μL CSF can be obtained from each mouse. **(B)** Scatter plot of the maximum ECL signal of the CSF assay of C57BL6 wild-type mice and APP/PS1 transgenic AD model mice with the pBPE-ECL system and significant difference analysis; data are shown as the mean ± SD (n = 5). P-values were determined by Student's t-test. ***P < 0.005. **(C, D)** Western blot analysis of Aβ oligomer level in APP/PS1 transgenic mice and age-matched C57/BL6 wild-type (WT) littermate mice at 6 month of age. Data represent the means ± SEM for five mice per group. ** P < 0.01 versus WT mice.

Potential application for Aβ(1–42) aggregation inhibitor screening

Encouraged by the excellent performance of the pBPE-ECL assay system in Aβ(1–42) aggregation analysis with APP/PS1 AD model mice, we next investigated its potential application to Aβ(1–42) aggregation inhibitor screening. Since Aβ(1–42) plays an important role in AD, agents that can suppress Aβ(1–42) aggregation hold promise as potential anti-AD drugs; therefore, it is of great importance to develop fast and reliable assays for high-throughput screening of compounds for Aβ(1–42) aggregation inhibition and investigation of their inhibitory effects. Here, two compounds proven to inhibit Aβ(1–42) aggregation were employed as models: Congo red (CR) and curcumin [3, 41]. CR could bind to the Aβ aggregation core region (Aβ16-20, KLVFF), inhibiting the β folding of Aβ and Aβ(1–42) aggregation [42] (**Figure 5A**), while curcumin could interact with the aromatic residues in the Aβ sequence, forcing these inhibitors into the center of the Aβ amino acid sequence and interfering with the aggregation of Aβ [43] (**Figure 5B**). Different concentrations of CR and curcumin ranging from 0 to 100 μM mixed with 50 nM Aβ(1–42) monomer were incubated at 37 °C in 5 mM pH 7.4 PBS solution for 24 h. The inhibited Aβ(1–42) aggregates were then incubated with 10 μM $[Ru(phen)_2dppz]^{2+}$ and 50 mM TPrA for 30 min and applied to the pBPE-ECL platform for ECL detection. As shown in **Figure 5C-D**, the ECL density decreased with increasing CR or curcumin concentration. The reduced ECL intensities suggested that Aβ(1–42) aggregation was significantly inhibited by both compounds. The relative Aβ(1–42) aggregation was further plotted as a function of inhibitor concentration and fitted with an exponential function. The IC_{50} values (half-maximal inhibitory concentration) of CR and curcumin were then determined to be 1.067 μM and 3.515 μM, respectively, which are close to the values reported previously [42, 43]. These values can help determine the inhibitory effect of these two kinds of inhibitors. A thioflavin T assay was also employed to verify the presence of amyloid-β oligomer/fibrils during Aβ(1–42) aggregation inhibitor screening. The experimental results in **Figure S7A-B** well verified the presence of amyloid-β oligomer/fibrils. Compared with other fluorescence- or electrochemistry-based screening methods, the pBPE-ECL assay system is more rapid and lower cost and does not require

expensive instruments or sophisticated operations [44, 45]. A comparison of the proposed ECL methods for Aβ(1-42) detection with other existing methods is presented in **Table S1**. The running cost of each of the fabricated pBPEs is estimated to be $0.005 (including conductive carbon ink, filter paper and wax). Note that the plastic support can be used repeatedly, and thus, its cost is negligible. In addition, the cost of reagents (such as TPrA and $[Ru(phen)_2dppz]^{2+}$) for each assay is approximately $0.3 since a small amount of reagents are needed in a test. More importantly, the pBPE is disposable and so amenable to batch fabrication that it can be considered a potential platform for rapid and high-throughput initial screening of Aβ(1–42) aggregation inhibitors as anti-AD drug agents. Before the pBPE-ECL device can be widely used in both laboratories and low-resource settings, however, further developments and improvements are required. A more integrated and portable app coupled with the assay system may make the system more conveniently utilized in conjunction with widely used mobile phones in the future. More importantly, multiple-test pBPE chips and standard internal reference samples may be developed for more precise and personalized diagnoses.

Conclusion

In this study, we constructed a pBPE-ECL platform to achieve label-free, real-time and rapid detection of the Alzheimer's disease biomarker Aβ(1-42) by taking advantage of the light-switch principle of the $[Ru(phen)_2dppz]^{2+}$ molecule in the presence of different forms of Aβ(1-42). This platform can smartly differentiate the presence and absence of Aβ(1-42) aggregates. The Aβ(1-42) aggregation process can also be monitored in real time by this system. This platform not only could detect as low as 100 pM equivalent monomer concentration of Aβ(1-42) in pure samples but also was capable of testing the CSF from transgenic AD model mice as an actual sample, providing results that are highly consistent with those of genetic identification. In addition, we demonstrated the feasibility of this platform as a potential new method for the screening of Aβ(1-42) aggregation inhibitors. By showing the ability of the pBPE-ECL system to rapidly and sensitively detect amyloid-β oligomerization without requiring expensive instruments or complex operations, we demonstrated the potential of this platform for AD diagnosis.

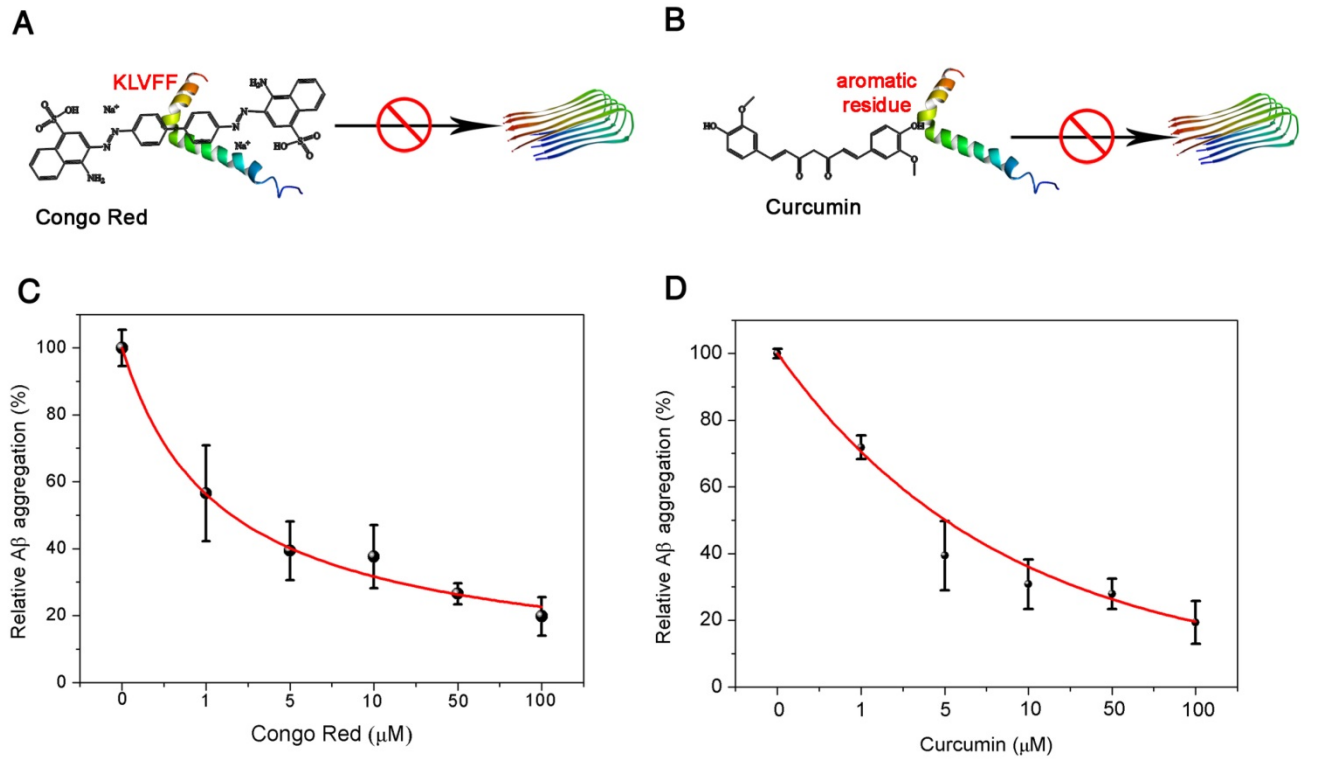

Figure 5. Potential application of the pBPE-ECL system to Aβ(1–42) aggregation inhibitor screening. (A) Congo red could bind to the Aβ(1–42) aggregation core region (Aβ16-20, KLVFF) and inhibit Aβ(1–42) aggregation by inhibition of β folding. **(B)** Curcumin could interact with the aromatic residues in the Aβ sequence, forcing the inhibitors into the center of the Aβ amino acid sequence and interfering with the aggregation of Aβ(1–42). The relative Aβ(1–42) aggregation is plotted as a function of inhibitor concentration. Aβ(1–42) (50 nM) was incubated at 37 °C in 5 mM pH 7.4 PBS solution for 24 h with different concentrations of **(C)** Congo red and **(D)** curcumin ranging from 0 to 100 μM.

Abbreviations

AD: alzheimer's disease; AFM: atomic force microscopy; AIE: aggregation-induced emission; CR: congo red; CSF: cerebrospinal fluid; CT: computerized x-ray tomography; ECL: electrochemiluminescence; ELISA: enzyme-linked immunosorbent assay; FCS: fluorescence correlation spectroscopy; LOD: limit of detection; MRI: magnetic resonance imaging; PAGE: polyacrylamide gel electrophoresis; pBPE-ECL: paper-based bipolar electrode electrochemiluminescence; SPR: surface plasmon resonance; ThT: thioflavin T; TPrA: Tripropylamine.

Supplementary Material

Supplementary figures and tables.
http://www.thno.org/v08p2289s1.pdf

Acknowledgments

This work was supported by the National Natural Science Foundation of China [Grant 21475048], the National Science Fund for Distinguished Young Scholars of Guangdong Province [Grant 2014A030306008], the Project of Guangzhou Science and Technology Plan [Grant 201508020003], the Program of the Pearl River Young Talents of Science and Technology in Guangzhou [Grant 2013J2200021], the Special Support Program of Guangdong Province (Grant 2014TQ01R599), and the Outstanding Young Teacher Training Program of Guangdong Province (Grant HS2015004). We give special thanks to Professor Caiping Tan from the School of Chemistry and Chemical Engineering, Sun Yat-Sen University, for help with synthesis and characterization of $[Ru(phen)_2dppz]^{2+}(PF6^-)^{2+}$.

Competing Interests

The authors have declared that no competing interest exists.

References

1. Querfurth HW, LaFerla FM. Alzheimer's Disease. N Engl J Med. 2010; 362: 329-44.
2. Liu Y, Yang Y, Sun M, Cui M, Fu Y, Lin Y, et al. Highly specific noninvasive photoacoustic and positron emission tomography of brain plaque with functionalized croconium dye labeled by a radiotracer. Chem Sci. 2017; 8: 2710-6.
3. Lee SJC, Nam E, Lee HJ, Savelieff MG, Lim MH. Towards an understanding of amyloid-[small beta] oligomers: characterization, toxicity mechanisms, and inhibitors. Chem Soc Rev. 2017; 46: 310-23.
4. Kaushik A, Jayant RD, Tiwari S, Vashist A, Nair M. Nano-biosensors to detect beta-amyloid for Alzheimer's disease management. Biosens Bioelectron. 2016; 80: 273-87.
5. Hampel H, Frank R, Broich K, Teipel SJ, Katz RG, Hardy J, et al. Biomarkers for Alzheimer's disease: academic, industry and regulatory perspectives. Nat Rev Drug Discov. 2010; 9: 560-74.
6. Porteri C, Albanese E, Scerri C, Carrillo MC, Snyder HM, Martensson B, et al. The biomarker-based diagnosis of Alzheimer's disease. 1—ethical and societal issues. Neurobiol Aging. 2017; 52: 132-40.
7. Zhou Y, Liu L, Hao Y, Xu M. Detection of Aβ Monomers and Oligomers: Early Diagnosis of Alzheimer's Disease. Chem Asian J. 2016; 11: 805-17.
8. Erkinjuntti T, Ketonen L, Sulkava R, Sipponen J, Vuorialho M, Iivanainen M. Do white matter changes on MRI and CT differentiate vascular dementia from Alzheimer's disease? J Neurol Neurosurg Psychiatry. 1988; 51: 318-9.
9. Pitschke M, Prior R, Haupt M, Riesner D. Detection of single amyloid [beta]-protein aggregates in the cerebrospinal fluid of Alzheimer's patients by fluorescence correlation spectroscopy. Nat Med. 1998; 4: 832-4.
10. Xia N, Liu L, Harrington MG, Wang J, Zhou F. Regenerable and Simultaneous Surface Plasmon Resonance Detection of Aβ(1−40) and Aβ(1−42) Peptides in Cerebrospinal Fluids with Signal Amplification by Streptavidin Conjugated to an N-Terminus-Specific Antibody. Anal Chem. 2010; 82: 10151-7.
11. Hong Y, Meng L, Chen S, Leung CWT, Da L-T, Faisal M, et al. Monitoring and Inhibition of Insulin Fibrillation by a Small Organic Fluorogen with Aggregation-Induced Emission Characteristics. J Am Chem Soc. 2012; 134: 1680-9.
12. Kwok RTK, Leung CWT, Lam JWY, Tang BZ. Biosensing by luminogens with aggregation-induced emission characteristics. Chem Soc Rev. 2015; 44: 4228-38.
13. Pujolpina R, Mazzucato R, Arcella A, Vilaseca M, Orozco M, Carulla N. SDS-PAGE analysis of Aβ oligomers is disserving research into Alzheimer´s disease: appealing for ESI-IM-MS. Sci Rep. 2015; 5: 14809.
14. Portelius E, Brinkmalm G, Ai JT, Zetterberg H, Westmanbrinkmalm A, Blennow K. Identification of Novel APP/Aβ Isoforms in Human Cerebrospinal Fluid. Neurodegener Dis. 2009; 6: 87-94.
15. Zhang Y, Rempel DL, Zhang J, Sharma AK, Mirica LM, Gross ML. Pulsed hydrogen-deuterium exchange mass spectrometry probes conformational changes in amyloid beta (Aβ) peptide aggregation. Proc Natl Acad Sci USA. 2013; 110: 14604-9.
16. Heo CH, Sarkar AR, Baik SH, Jung TS, Kim JJ, Kang H, et al. A quadrupolar two-photon fluorescent probe for in vivo imaging of amyloid-[small beta] plaques. Chem Sci. 2016; 7: 4600-6.
17. Munishkina LA, Fink AL. Fluorescence as a method to reveal structures and membrane-interactions of amyloidogenic proteins. Biochim Biophys Acta. 2007; 1768: 1862-85.
18. Levine H. Thioflavine T interaction with synthetic Alzheimer's disease beta-amyloid peptides: detection of amyloid aggregation in solution. Protein Sci. 1993; 2: 404-10.
19. Golde TE, Eckman CB, Younkin SG. Biochemical detection of Aβ isoforms: implications for pathogenesis, diagnosis, and treatment of Alzheimer's disease. BBA-Mol Basis Dis. 2000; 1502: 172-87.
20. Yu Y, Zhang L, Li C, Sun X, Tang D, Shi G. A Method for Evaluating the Level of Soluble β-Amyloid(1–40/1–42) in Alzheimer's Disease Based on the Binding of Gelsolin to β-Amyloid Peptides. Angew Chem Int Ed Engl. 2014; 53: 12832-5.
21. Zhou Y, Zhang H, Liu L, Li C, Chang Z, Zhu X, et al. Fabrication of an antibody-aptamer sandwich assay for electrochemical evaluation of levels of β-amyloid oligomers. Sci Rep. 2016; 6: 35186.
22. Liu H, Zhou X, Liu W, Yang X, Xing D. Paper-Based Bipolar Electrode Electrochemiluminescence Switch for Label-Free and Sensitive Genetic Detection of Pathogenic Bacteria. Anal Chem. 2016; 88: 10191-7.
23. Cook NP, Torres V, Jain D, Martí AA. Sensing Amyloid-β Aggregation Using Luminescent Dipyridophenazine Ruthenium(II) Complexes. J Am Chem Soc. 2011; 133: 11121-3.
24. Aliyan A, Kirby B, Pennington C, Martí AA. Unprecedented Dual Light-Switching Response of a Metal Dipyridophenazine Complex toward Amyloid-β Aggregation. J Am Chem Soc. 2016; 138: 8686-9.
25. Cook NP, Ozbil M, Katsampes C, Prabhakar R, Martí AA. Unraveling the Photoluminescence Response of Light-Switching Ruthenium(II) Complexes Bound to Amyloid-β. J Am Chem Soc. 2013; 135: 10810-6.
26. Li M, Howson SE, Dong K, Gao N, Ren J, Scott P, et al. Chiral Metallohelical Complexes Enantioselectively Target Amyloid β for Treating Alzheimer's Disease. J Am Chem Soc. 2014; 136: 11655-63.
27. Hayne DJ, Lim S, Donnelly PS. Metal complexes designed to bind to amyloid-[small beta] for the diagnosis and treatment of Alzheimer's disease. Chem Soc Rev. 2014; 43: 6701-15.
28. Hu L, Bian Z, Li H, Han S, Yuan Y, Gao L, et al. [Ru(bpy)2dppz]2+ Electrochemiluminescence Switch and Its Applications for DNA Interaction Study and Label-free ATP Aptasensor. Anal Chem. 2009; 81: 9807-11.
29. Li M, Guan Y, Zhao A, Ren J, Qu X. Using Multifunctional Peptide Conjugated Au Nanorods for Monitoring β-amyloid Aggregation and Chemo-Photothermal Treatment of Alzheimer's Disease. Theranostics. 2017; 7: 2996-3006.
30. Shi H-W, Wu M-S, Du Y, Xu J-J, Chen H-Y. Electrochemiluminescence aptasensor based on bipolar electrode for detection of adenosine in cancer cells. Biosens Bioelectron. 2014; 55: 459-63.
31. Feng Q-M, Pan J-B, Zhang H-R, Xu J-J, Chen H-Y. Disposable paper-based bipolar electrode for sensitive electrochemiluminescence detection of a cancer biomarker. Chem Commun. 2014; 50: 10949-51.
32. Costa MN, Veigas B, Jacob JM, Santos DS, Gomes J, Baptista PV, et al. A low cost, safe, disposable, rapid and self-sustainable paper-based platform for diagnostic testing: lab-on-paper. Nanotechnology. 2014; 25: 094006.
33. Martinez AW, Phillips ST, Whitesides GM, Carrilho E. Diagnostics for the Developing World: Microfluidic Paper-Based Analytical Devices. Anal Chem. 2010; 82: 3-10.

34. Guan Y, Li M, Dong K, Gao N, Ren J, Zheng Y, et al. Ceria/POMs hybrid nanoparticles as a mimicking metallopeptidase for treatment of neurotoxicity of amyloid-β peptide. Biomaterials. 2016; 98: 92-102.
35. Liu L, Herukka S-K, Minkeviciene R, van Groen T, Tanila H. Longitudinal observation on CSF Aβ42 levels in young to middle-aged amyloid precursor protein/presenilin-1 doubly transgenic mice. Neurobiol Dis. 2004; 17: 516-23.
36. Liu M, Liu R, Wang D, Liu C, Zhang C. A low-cost, ultraflexible cloth-based microfluidic device for wireless electrochemiluminescence application. Lab Chip. 2016; 16: 2860-70.
37. Wu M-S, Yuan D-J, Xu J-J, Chen H-Y. Electrochemiluminescence on bipolar electrodes for visual bioanalysis. Chem Sci. 2013; 4: 1182-8.
38. Wang S, Ge L, Song X, Yu J, Ge S, Huang J, et al. Paper-based chemiluminescence ELISA: Lab-on-paper based on chitosan modified paper device and wax-screen-printing. Biosens Bioelectron. 2012; 31: 212-8.
39. Lopes P, Xu M, Zhang M, Zhou T, Yang Y, Wang C, et al. Direct electrochemical and AFM detection of amyloid-[small beta] peptide aggregation on basal plane HOPG. Nanoscale. 2014; 6: 7853-7.
40. Zhou Y, Dong H, Liu L, Xu M. Simple Colorimetric Detection of Amyloid β-peptide (1–40) based on Aggregation of Gold Nanoparticles in the Presence of Copper Ions. Small. 2015; 11: 2144-9.
41. Ma DL, Chan DS, Ma VP, Leung KH, Zhong HJ, Leung CH. Current advancements in Aβ luminescent probes and inhibitors of Aβ aggregation. Curr Alzheimer Res. 2012; 9: 830-43.
42. Lorenzo A, Yankner BA. β-Amyloid Neurotoxicity Requires Fibril Formation and is Inhibited by Congo Red. Proc Natl Acad Sci USA. 1994; 91: 12243-7.
43. Ono K, Hasegawa K, Naiki H, Yamada M. Curcumin has potent anti-amyloidogenic effects for Alzheimer's beta-amyloid fibrils in vitro. J Neurosci Res. 2004; 75: 742-50.
44. Nie Q, Du X-g, Geng M-y. Small molecule inhibitors of amyloid [beta] peptide aggregation as a potential therapeutic strategy for Alzheimer's disease. Acta Pharmacol Sin. 2011; 32: 545-51.
45. Wang Q, Yu X, Li L, Zheng J. Inhibition of Amyloid-beta Aggregation in Alzheimer's Disease. Curr Pharm Des. 2014; 20: 1223-43.